Fluctuations in radioactive decays. II. Experimental results

Roberto Boscaino and Giorgio Concas
Dipartimento di Scienze Fisiche, Università di Cagliari, via Ospedale 72, I-09124 Cagliari, Italy

Marcello Lissia
Istituto Nazionale di Fisica Nucleare, via Negri 18, I-09127 Cagliari, Italy

Sergio Serci
Dipartimento di Scienze Fisiche, Università di Cagliari, via Ospedale 72, I-09124 Cagliari, Italy and Istituto Nazionale di Fisica Nucleare, via Negri 18, I-09127 Cagliari, Italy
(Received 2 August 1993)

We experimentally investigate the decay statistics of a γ source of $^{119m}_{50}$Sn. We find that, for counting periods of the order of 10 h, the variance is higher than the Poissonian value by more than one order of magnitude. A careful study of the relative Allan variance and the measurement of the generalized Allan variance demonstrates that the observed anomaly is not caused by $1/f$ noise. Rather, even if counting periods are much shorter than the nucleus lifetime, the variance excess is a consequence of the nonequilibrium nature of the decay process. This conclusion is supported by the quantitative agreement between our experimental data and the theoretical formulas derived in the preceding paper [Boscaino *et al.*, Phys. Rev. E **49**, 333 (1994)].

PACS number(s): 05.40.+j, 23.20.−g, 02.50.−r, 29.90.+r

I. INTRODUCTION

The decay of nuclei through the emission of particles or radiation is often cited as an archetype of the simple Poisson process, since the unit-time probability of the decay events is time independent and the events are uncorrelated from each other. Nevertheless, in the past decade, it has been conjectured that the statistics of the particle counting in a nuclear decay experiment could deviate from the pure Poisson behavior because of the existence of additional sources of fluctuations superimposed onto the intrinsic shot noise: essential $1/f$ noise of the emission rate, Lorentzian noise, originating from cooperative effects, and other detector-related nontrivial noise sources, e.g., solid angle fluctuations and spatial $1/f$ noise in track detectors [1–7].

In the past ten years, many authors have studied experimentally the counting statistics of emitted particles or photons and compared their results to the standard Poisson theory. Results have been conflicting even for the same type of source. Experiments on α sources ($^{241}_{95}$Am [8–10] and $^{210}_{84}$Po [11]) and on a β source of $^{137}_{55}$Cs [12] have confirmed the Poissonian nature of these decay processes. Conversely, a counting variance in excess of the Poisson value had been measured, for long counting periods, in experiments on the α decay of $^{241}_{95}$Am, $^{239}_{94}$Pu, and $^{244}_{96}$Cm [7,13–15] and on the β decay of $^{204}_{81}$Tl and $^{90}_{39}$Y [16,17].

In the preceding paper [18], hereafter referred to as I, we have shown theoretically that the statistics of the decay, as measured by counting the particles emitted by a system of N decaying centers in a given period T, reveal an additional contribution to the variance due to the exponential decrease of N in time. The relevant feature of this contribution is that it manifests itself even for counting periods T much shorter than the nuclear lifetime. As shown in I, this aspect has been overlooked [8,9,11–14,16,17] or underestimated [10,15] in previous investigations.

The present paper is intended as the experimental counterpart to I. We report experimental results on the statistics of the $^{119m}_{50}$Sn nuclear decay. We find that the relative Allan variance of the emitted γ-photon counts, for periods longer than a few hours, is higher than the Poisson value, and the excess ratio amounts to more than one order of magnitude for periods of the order of 10 h. The agreement between our experimental results and the theory derived in I is quantitative, thus strongly supporting our explanation of the phenomenon [19]: the nonequilibrium nature of the decay process is responsible for the excess of variance.

In Sec. II we describe the source and the experimental apparatus. The experimental results and their statistical analysis are reported in Sec. III, where the comparison with the theoretical predictions is also carried out. Finally, Sec. IV is reserved for our conclusions.

II. EXPERIMENTAL SETUP

A. The source

In our experiments we use a crystal of $CaSnO_3$ containing $^{119m}_{50}$Sn nuclei. These nuclei are in a metastable state with an energy of 89.5 keV above the ground state and a lifetime $\tau = 422.7$ days [20,21]. The decay scheme of the nucleus from the excited to the ground state is shown in the inset of Fig. 1 [20]. The first step is an isomeric

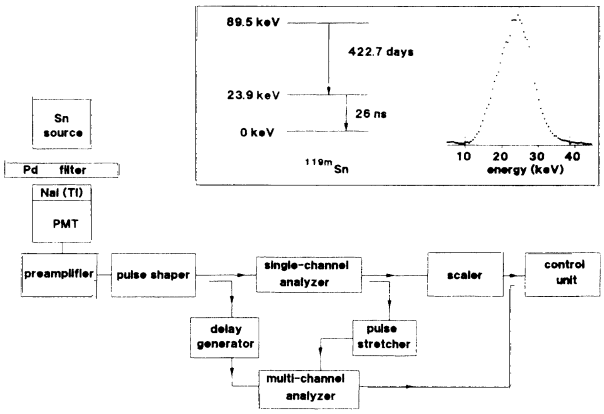

FIG. 1. Block diagram of the experimental apparatus. The decay scheme of $^{119m}_{50}$Sn and the energy spectrum of the detected radiation are shown in the inset.

transition to an intermediate state with energy 23.9 keV and lifetime 26 ns. This magnetic octupole transition occurs mainly through the emission of electrons, with a ratio between number of emitted electrons and number of emitted γ photons (coefficient of internal conversion) $\alpha = 4999$. The emission of atomic electrons causes a secondary production of x photons, especially $K\alpha_1$ (energy 25.0 keV, probability 8%), $K\alpha_2$ (energy 25.3 keV, probability 15%) and $K\beta_1$ (energy 28.5 keV, probability 4%) [21]. The second step of the decay is a magnetic dipole transition from the intermediate to the ground state with a coefficient of conversion $\alpha = 5.21$, corresponding to a 16% probability of emission of 23.9 keV γ photons per decay.

In our experiments we are interested in the counting statistics of the 23.9 keV photons emitted during the second step of the decay. The lifetime of this intermediate state (26 ns) is much shorter than both the lifetime of the initial metastable state ($\tau = 422.7$ days) and the shortest counting period we consider (1 ms); therefore, we can safely assume that the measured statistics coincide, for all practical purposes, with those of the decay from the initial metastable state.

B. Experimental apparatus and procedure

A schematic of the experimental apparatus is shown in Fig. 1. The radioactive source (activity approximately 1.3 MBq) is shaped as a thin disk, 16 mm in diameter. A thin foil of Pd is inserted between the source and the detector to filter away x photons. The γ photons are detected by a NaI(Tl) crystal, shaped as a disk with a 50 mm diameter and 2 mm thick; the crystal is protected by a 0.12 mm thick Be window. The detector is integrally mounted on a photomultiplier tube (PMT). The source and the detector are coaxially mounted and mechanically fixed at a distance of a few centimeters.

The output signal from the PMT, after preamplification in the PMT base, is amplified by a spectroscopy amplifier and shaped to unipolar Gaussian pulse, with a shaping time constant of 0.5 μs. Finally, it is processed by a single-channel analyzer (SCA), which selects those pulses whose amplitude corresponds to a preselected energy window. The SCA outputs transistor-transistor logic pulses with a width of 0.5 μs; the resolving time for successive pulses is 0.6 μs. Counting is performed by a programmable multi-channel scaler board installed on an IBM personal computer (PC). The dead time of the whole system is (2.5 ± 0.6) μs, as determined by the standard two-source method [22]. This value is low enough to ensure that the system works far from saturation at 5500 counts per second, the highest counting rate in our experiments.

We prepared the experiments by measuring the photon energy spectrum with a multichannel analyzer (MCA) board mounted on the PC. The MCA performs pulse-height analysis of the output signal of the shaping amplifier, using the stretched output of the SCA as gate signal. We then selected the energy window from 10 keV to 38 keV; the resulting photon energy spectrum is shown in the inset of Fig. 1. Given the length of our experiments, the first run lasted about 40 days and the second one twice as long, it is important to verify the stability of the energy window. Therefore, we measured the energy spectrum also at the end of each run and found no detectable drift of the energy window. Since our apparatus is not thermalized, temperature variations might bring correlated variations of the PMT efficiency which in turn could induce spurious fluctuations in the number of counts. However, we examined the time sequence of the counting data and their time correlations and we find no measurable effect due to the daily temperature variations. The only source of drift of the detection apparatus that we were able to measure on the time scale of the experiment is the slow aging of the PMT. The effect of this slow drift will be examined at the end of Sec. III. There we shall also present the data analysis that can be used to correct this instrumental effect. However, we apply this correction only to the data shown in the following Fig. 5. All the statistics shown in the other figures and discussed in the text use the raw uncorrected count data.

The system is fully programmable. The PC provides for automatic control of the whole experiment and data storage, thus allowing continuous unattended data collection. We describe here two experiments carried out with the same source but at two different counting rates. For each experiment, a set of six values of the basic counting period T_b is prefixed in the control program: 1 ms, 10 ms, 100 ms, 1 s, 10 s, and 100 s. For each value of T_b, starting from the shortest one, the system performs 4032 counting measures and group them as follows: the first 64 are taken as 64 measures at $T = T_b$, the successive 128 are taken as 64 measures at $T = 2T_b$, and so on up to $T = 32T_b$. The same procedure is repeated for all the values of T_b from 1 ms to 10 s. For $T_b = 100$ s, 32 704 measures are performed and the same grouping procedure is extended up to $T = 256T_b$. Counting data are periodically saved on hard disk. At the end of the first run, which lasted nearly 40 days, results were available as 39 sequences of $n = 64$ counts taken at various values of the counting period T, ranging from 1 ms up to 2.56×10^4 s. In the latter of our two runs, which lasted about 80 days,

we performed 65 472 measures at $T_b = 100$ s, in order to extend the range of T up to 5.12×10^4 s.

We emphasize that in our procedure no use is made of *add-up* methods, frequently used in previously reported experiments [8,10,11,13–17], to save data acquisition time. Therefore, our count data are truly statistically independent: each one originates from a different measure.

III. RESULTS AND DISCUSSION

We report results from two experiments carried out using the same γ source but different counting rates. For the first experiment, we located the source at 35 mm from the detector and measured a counting rate $r = 5500$ counts per second; for the second experiment we located the source at 75 mm from the detector reducing the rate to $r = 1300$ counts per seconds.

The output of each experiment consists of sequences $M_k(T)$ of n ($k = 0, \ldots, n-1$) counts, at various values of the counting period T; we consistently used $n = 64$. Following the usual procedure, we characterize the counting statistics by evaluating, at each value of T, the relative Allan variance R [4,23–25], which is defined as

$$R(T) \equiv \frac{A_n^2(T)}{[\overline{M}_n(T)]^2} \quad , \tag{1}$$

where $\overline{M}_n(T)$ is the average count over n consecutive intervals

$$\overline{M}_n(T) \equiv \frac{1}{n} \sum_{k=0}^{n-1} M_k(T) \tag{2}$$

and $A_n^2(T)$ is the corresponding Allan variance

$$A_n^2(T) \equiv \frac{1}{2(n-1)} \sum_{k=0}^{n-2} [M_k(T) - M_{k+1}(T)]^2 \quad . \tag{3}$$

A pure Poisson process would have an Allan variance $A_n^2(T) = \overline{M}_n(T)$ and, therefore, the reduced Allan variance would depend linearly on $\frac{1}{T}$: $R(T) = \frac{1}{\overline{M}_n(T)} = \frac{1}{r_n T}$. We find it convenient to define the average counting rate $r_n = \frac{\overline{M}_n(T)}{T}$. Contrary to this expectation, the theory presented in I gives the following dependence of the reduced variance R on T:

$$R(T) = \frac{1}{r_n T} + \frac{1}{2} \left(\frac{T}{\tau} \right)^2 \quad , \tag{4}$$

where τ is the lifetime of the nucleus. In I, the corresponding formulas contained the expected values of the average count, average rate and variance. Here we use the measured ones: the difference is of higher order in T/τ and then negligible.

Results of our first experiment ($r = 5500$ counts per seconds) are reported in Fig. 2, where the measured values of R are plotted versus $1/T$ on a logarithmic scale. We emphasize that all data points reported in Fig. 2 originate from the same uninterrupted run and each one

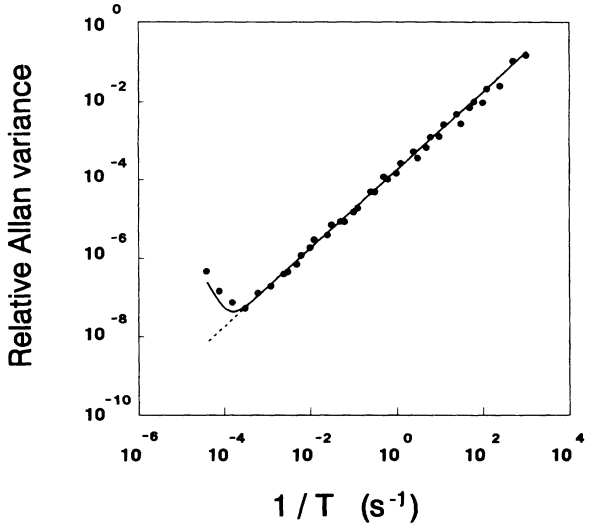

FIG. 2. Relative Allan variance R versus $1/T$, as obtained in our first experiment, which had a rate of 5500 counts per second. Dots are the experimental values. The dashed line plots the Poisson behavior. The full curve plots the theoretical dependence given by Eq. (4).

was determined from independent count data. Moreover, variances at every value of T were obtained using the same number $n = 64$ of count data, so that they have the same percentage statistical uncertainty. For the sake of comparison, we also plot in Fig. 2 the dependence of R on $1/T$ expected for a stationary Poisson process (dashed line). The experimental points follow the Poisson curve for $T < 3000$ s, whereas for longer values of T the measured variance is higher than naively expected. R takes its minimum value $R_{\min}^{\text{expt}} = (5 \pm 2.5) \times 10^{-8}$ at $T_{\min}^{\text{expt}} = (5 \pm 2) \times 10^3$ s and then increases with T. At the longest counting period we explored, $T = 2.56 \times 10^4$ s, the experimental value of R is higher than the Poisson expected value by a factor of 70, well above experimental and statistical uncertainties. Statistical uncertainties have been estimated by Monte Carlo simulation in I and confirmed by the actual spread of the data points around the curve.

The experimental dependence of R on T is in reasonable agreement with the theoretical formula derived in (I). Figure 2 clearly shows how well the experimental data agree with Eq. (4) plotted as a full line. In Eq. (4) we used the experimental rate $r_n = 5500$ s and the known lifetime of the metastable state $\tau = 423$ days [20,21]. The theory correctly predicts also the position of the minimum and the relative rate. In fact, the coordinates of the minimum predicted by Eq. (4) are

$$R_{\min} = \frac{3}{2} (r_n \tau)^{-\frac{2}{3}} \quad \text{at} \quad T_{\min} = \tau (r_n \tau)^{-\frac{1}{3}} \quad . \tag{5}$$

Substituting in the above formulas the experimental rate $r_n = 5500$ s and the lifetime $\tau = 423$ days [20,21] we find $R_{\min}^{\text{theor}} = 3.4 \times 10^{-8}$ and $T_{\min}^{\text{theor}} = 6.3 \times 10^3$ s; these values are consistent with the ones estimated from the experimental points: $R_{\min}^{\text{expt}} = (5 \pm 2.5) \times 10^{-8}$ and

$T_{\min}^{\text{expt}} = (4 \pm 2) \times 10^3$ s. In spite of the overall agreement between the experimental data shown in Fig. 2, we wish to point out that the systematic discrepancy between the experimental points and the theoretical curve (full line) for for $T > T_{\min}$ cannot be explained by the statistical uncertainties. In fact, according to Monte Carlo simulations of the experiment, whose results have been reported in Fig. 1 of I, the standard deviation of R is expected to be rather low in this range of T. The underlying physical reason is that the variance becomes more and more dominated by the exponential decay rather than by the statistical fluctuations. We shall address this discrepancy at the end of this section.

A further test of the theory reported in I is the dependence of $R_{\min}$ and $T_{\min}$ on the counting rate r. To check this dependence, we performed a second experiment: this time we located the same source farther away from the detector resulting in the lower rate $r = 1300$ counts per second. The values of R measured in the second experiment are plotted versus $1/T$ in Fig. 3(a). To compare this last set of data with the corresponding data obtained in the first experiment, in Fig. 3(b) we report the data from the first experiment on the same scale of the data from the second experiment. These same data had already been plotted in Fig. 2, but on a different scale. In agreement with Eq. (5) the lower counting rate r results in a higher minimum, $R_{\min}^{\text{expt}} = (1.5 \pm 0.7) \times 10^{-7}$, shifted towards longer counting periods, $T_{\min}^{\text{expt}} = (1.3 \pm 0.6) \times 10^4$ s; the corresponding values obtained from Eq. (5) $R_{\min}^{\text{theor}} = 1.1 \times 10^{-7}$ and $T_{\min}^{\text{theor}} = 1.0 \times 10^4$ s are again well within the experimental uncertainties.

Further statistical analysis of the counting data was carried out using the generalized relative Allan variance $R_G(T,j) \equiv \frac{G_n^2(T,j)}{[\bar{M}_n(T)]^2}$; the generalized Allan $G_n^2(T,j)$ variance was first introduced in I:

$$G_n^2(T,j) \equiv \frac{1}{2(n-j)} \sum_{k=0}^{n-1-j} [M_k - M_{k+j}]^2 \quad . \tag{6}$$

The analysis involves the j dependence of R_G at a fixed value of the counting period and, since we only show results for $T = 100$ s, from now on we shall simply write $R_G(j)$. We recall that for stationary process R_G is expected to be independent of j. Contrary to this expectation, we predicted in I that the effect of the decay would yield the following dependence of R_G on T:

$$R_G(j) = \frac{1}{r_n T} + \frac{j^2}{2}(T/\tau)^2 \quad . \tag{7}$$

In Fig. 4 we report R_G as a function of j^2. We used data from 30 000 consecutive 100 s measures taken from the first experiment. As predicted by Eq. (7), $R_G(j)$ depends linearly on j^2, but the slope is different from the predicted one. Best fitting of $R_G(j) = a + bj^2$ to the data points shown in Fig. 4 yields $b^{\text{expt}} = 7.1 \times 10^{-12}$, against the predicted value $b^{\text{theor}} = 3.7 \times 10^{-12}$. Since $b^{\text{theor}} = \frac{T^2}{2\tau^2}$, this discrepancy can be reformulated by saying that the experimental data of Fig. 4 are consistent with a decay time $\tau = 307$ days, to be contrasted to the nuclear lifetime $\tau = 423$ days [20,21].

To understand this discrepancy, we reexamined the count data obtained in the first experiment at $T = 100$ s as a function of time, over a time interval of nearly 40

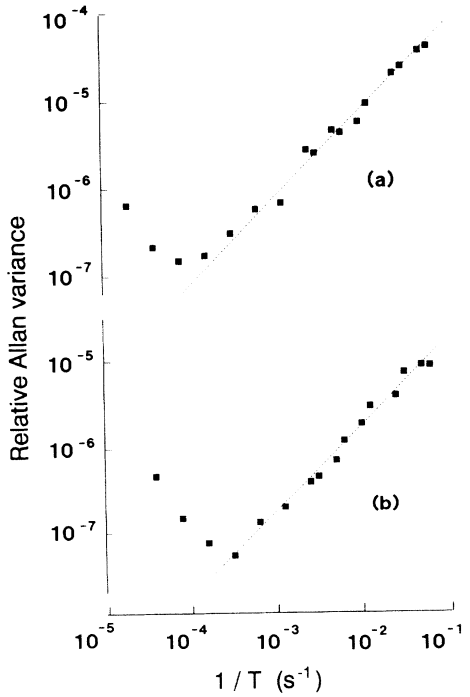

FIG. 3. Relative Allan variance R versus $1/T$, as obtained in (a) the second experiment with a rate of 1300 counts per second and (b) in the first experiment with a rate of 5500 counts per second. Dots are the experimental values. The dashed lines plot the Poisson behavior.

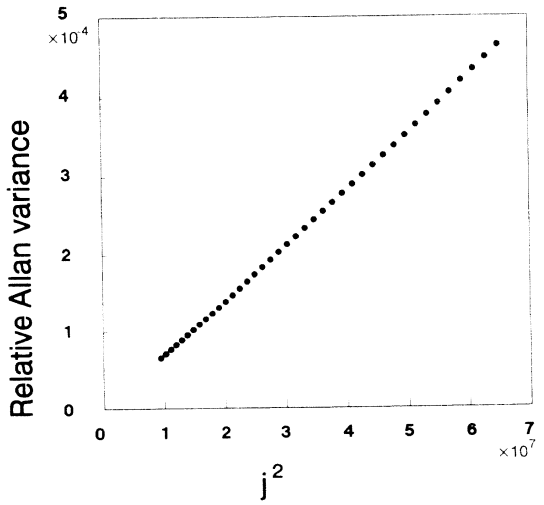

FIG. 4. Generalized relative Allan variance $R_G(j)$ versus j^2, as determined from the count data obtained in the first experiment. Data points are well fitted by a straight line (not shown) of equation $R = a + bj^2$ with $a = (-0.4 \pm 1.5) \times 10^{-6}$ and $b = (7.09 \pm 0.01) \times 10^{-12}$.

days. We found that this time series is consistent with an effective decay time $\tau_{\text{eff}} = (315 \pm 15)$ days: This value is 20% smaller than the known decay time. This discrepancy can be modeled by composing the nuclear decay with an additional decay with a lifetime $\tau' = 1235$ days, if we use the central value $\tau_{\text{eff}} = 315$ days; a possible source of this additional decay is the aging of the PMT. This additional decay due to the experimental apparatus also explains the minor deviation of data points in Fig. 1 from the full line; we stress that this line is not fitted to the data but calculated from independently measured parameters. As shown below, this exponential loss of efficiency of our experimental apparatus does not undermine the conclusions drawn above.

We can simulate an external feedback loop in the experimental setup that compensates the progressive reduction of efficiency of the PMT by scaling the original count data by the factor $\exp(t/\tau')$, where t is the time elapsed from the beginning of the experiment and $\tau' = 1235$ days; note that in this exercise we use the central value $\tau_{\text{eff}} = 315$ days. This is a sensible correction because the aging of the PMT is well described by an exponential; moreover, we are interested only in the fluctuations of the decay and can afford to renormalize parameters to their best experimental values. By repeating the statistical analysis on the renormalized data, we obtained the results shown in Fig. 5. The agreement between the theoretical prediction (full line) for R versus $1/T$ and the corresponding data after renormalization [Fig. 5(a)] is striking. The renormalization of the data has clearly improved the already good result shown in Fig. 2. In Fig. 5(b) we plot the renormalized values of R_G as a function of j^2 and compare them to the theoretical straight line resulting from Eq. (7). There is still some discrepancy due to the high sensitivity of the slope of the curve to the exact value of τ: a change $\Delta\tau$ in the mean life yields a percentage change in the slope $\frac{\Delta b}{b} = -\frac{2\Delta\tau}{\tau}$. Figure 5(b) shows a 8% discrepancy in the slope which corresponds to 4% error in the effective mean life.

As a matter of fact, there is no statistically significant discrepancy between the slope of the corrected data and the theoretical slope, once we take into account the uncertainty on the measure of τ_{eff}. It is a simple exercise to show that an error Δ_{eff} in the value of τ_{eff} yields the following change in the slope b:

$$b = b^{\text{theor}} \left[1 + \frac{\tau}{\tau_{\text{eff}} + \Delta_{\text{eff}}} \frac{\Delta_{\text{eff}}}{\tau_{\text{eff}}}\right]^2 .$$

The 5% uncertainty on the measured value of τ_{eff} implies a 13% uncertainty on the value of the slope. Given the high sensitivity of this slope to the exact value of τ_{eff}, we could have taken the opposite point of view. We could have found τ_{eff} as the value that best brings the corrected data in agreement with the theoretical curve. This procedure for measuring τ_{eff} would have produced a much smaller error on τ_{eff}. Moreover, the already very good agreement of the corrected data with the theoretical curve in Fig. 5(a) would have become practically perfect.

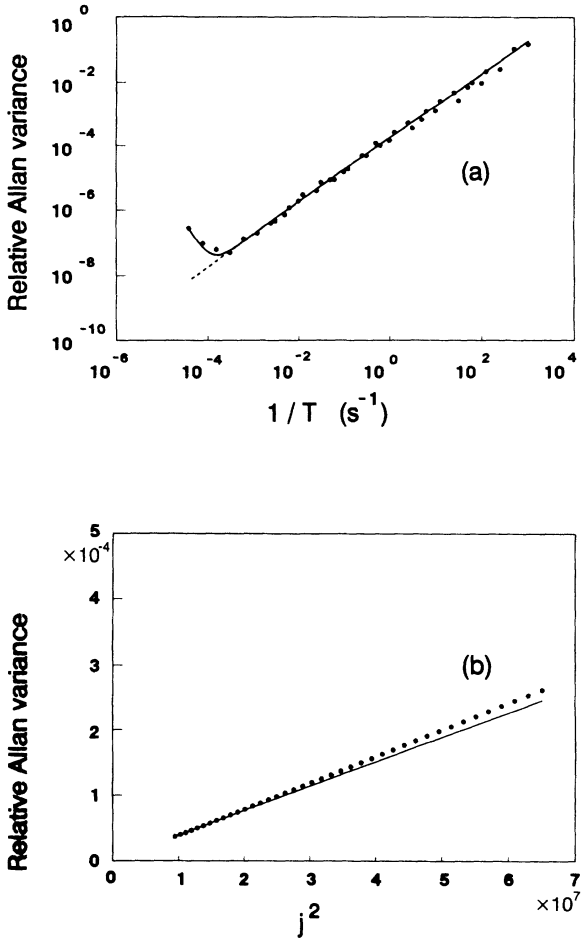

FIG. 5. Statistical analysis of the count data obtained in the first experiment after the correction discussed in the text: (a) R versus $1/T$ and (b) R_G versus j^2. The straight line in (b) plots the theoretical dependence given by Eq. (7)

IV. CONCLUSIONS

We have reported experimental results on the decay statistics of a γ source; careful measurements of these statistics require several months of data acquisition. At long counting periods, we have found values of the counting variance much higher than the ones expected for a stationary Poisson process. This departure is closely similar to the superstatistical emission noise measured in earlier work [7,13–17] aimed at detecting flicker noise in nuclear decays. However, we have shown that the observed non-Poissonian behavior of the Allan variance, at least in our measures, is not indicative of $1/f$ noise. Rather it is related to the circumstance that the number of emitters is decreasing and, therefore, the decay is not a stationary process. This conclusion is supported by the statistical analysis carried out in terms of the relative Allan variance and by the quantitative agreement with the theoretical formulas obtained in I.

Moreover, we used for the first time, to the best of our knowledge, the generalized Allan variance, which we introduced in I [18]. We have verified that its dependence on j is very sensitive to physical and instrumental drifts. We believe that this correlation deserves to be considered as an experimental tool for monitoring spurious drifts or, perhaps, for measuring physical ones.

ACKNOWLEDGMENTS

We are grateful to C. Muntoni for stimulating and encouraging discussions on the subject of the present work. Financial support has been given by Italian Ministry of University and Research and by Istituto Nazionale di Fisica Nucleare.

[1] P. H. Handel, Phys. Rev. Lett. **34**, 1492 (1975).
[2] P. H. Handel, Phys. Rev. Lett. **34**, 1495 (1975).
[3] P. H. Handel, Phys. Rev. A **22**, 745 (1980).
[4] C. M. V. Vliet, P. H. Handel, and A. V. der Ziel, Physica A **108**, 511 (1981).
[5] C. M. V. Vliet and P. H. Handel, Physica A **113**, 261 (1982).
[6] C. M. V. Vliet, Solid State Electron. **34**, 1 (1991).
[7] V. D. Rusov *et al.*, Nucl. Tracks Radiat. Meas. **20**, 305 (1992).
[8] W. V. Prestwich, T. J. Kennett, and G. T. Pepper, Phys. Rev. A **34**, 5132 (1986).
[9] G. T. Pepper, T. J. Kennett, and W. V. Prestwich, Can. J. Phys. **67**, 468 (1989).
[10] T. J. Kennett and W. V. Prestwich, Phys. Rev. A **40**, 4630 (1989).
[11] M. A. Azhar and K. Gopala, Phys. Rev. A **39**, 5311 (1989).
[12] K. Gopala and M. A. Azhar, Phys. Rev. A **37**, 2173 (1988).
[13] J. Gong *et al.*, in *Noise in Physical Systems and 1/f Noise*, edited by M. Savelli, G. Lecoy, and J. P. Nougier (Elsevier, New York, 1983), p. 381.
[14] G. S. Kousik *et al.*, in *Noise in Physical Systems and 1/f Noise*, edited by A. D'Amico and P. Mazzetti (Elsevier, New York, 1986), p. 469.
[15] G. S. Kousik *et al.*, Can. J. Phys. **65**, 365 (1987).
[16] M. A. Azhar and K. Gopala, Phys. Rev. A **39**, 4137 (1989).
[17] M. A. Azhar and K. Gopala, Phys. Rev. A **44**, 1044 (1991).
[18] R. Boscaino, G. Concas, M. Lissia, and S. Serci, preceding paper, Phys. Rev. E **49**, 333 (1994).
[19] R. Boscaino, G. Concas, M. Lissia, and S. Serci, INFN Cagliari Preprint Report No. INFNCA93-BCLS1, 1993 (unpublished).
[20] R. L. Auble, Nucl. Data Sheets **26**, 207 (1979).
[21] E. Browne and R. B. Firestone, *Table of Radioactive Isotopes* (Wiley, New York, 1986).
[22] W. R. Leo, in *Techniques for Nuclear and Particle Physics Experiments* (Springer-Verlag, Berlin, 1987), Chap. 5, p. 116.
[23] J. A. Barnes, Proc. IEEE **54**, 207 (1966).
[24] D. W. Allan, Proc. IEEE **54**, 221 (1966).
[25] W. V. Prestwich, T. J. Kennett, and F. W. Kus, Can. J. Phys. **69**, 1405 (1991).